

Are your MRI contrast agents cost-effective?

Learn more about generic Gadolinium-Based Contrast Agents.



FRESENIUS  
KABI

caring for life

# AJNR

This information is current as  
of April 17, 2024.

## Brain MR Spectroscopic Findings in 3 Consecutive Patients with COVID-19: Preliminary Observations

O. Rapalino, A. Weerasekera, S.J. Moum, K.  
Eikermann-Haerter, B.L. Edlow, D. Fischer, A.  
Torrado-Carvajal, M.L. Loggia, S.S. Mukerji, P.W.  
Schaefer, R.G. Gonzalez, M.H. Lev and E.-M. Ratai

*AJNR Am J Neuroradiol* 2021, 42 (1) 37-41

doi: <https://doi.org/10.3174/ajnr.A6877>

<http://www.ajnr.org/content/42/1/37>

# Brain MR Spectroscopic Findings in 3 Consecutive Patients with COVID-19: Preliminary Observations

O. Rapalino, A. Weerasekera, S.J. Moun, K. Eikermann-Haerter, B.L. Edlow, D. Fischer, A. Torrado-Carvajal, M.L. Loggia, S.S. Mukerji, P.W. Schaefer, R.G. Gonzalez, M.H. Lev, and E.-M. Ratai



## ABSTRACT

**SUMMARY:** Brain multivoxel MR spectroscopic imaging was performed in 3 consecutive patients with coronavirus disease 2019 (COVID-19). These included 1 patient with COVID-19-associated necrotizing leukoencephalopathy, another patient who had a recent pulseless electrical activity cardiac arrest with subtle white matter changes, and a patient without frank encephalopathy or a recent severe hypoxic episode. The MR spectroscopic imaging findings were compared with those of 2 patients with white matter pathology not related to Severe Acute Respiratory Syndrome coronavirus 2 infection and a healthy control subject. The NAA reduction, choline elevation, and glutamate/glutamine elevation found in the patient with COVID-19-associated necrotizing leukoencephalopathy and, to a lesser degree, the patient with COVID-19 postcardiac arrest, follow a similar pattern as seen with the patient with delayed posthypoxic leukoencephalopathy. Lactate elevation was most pronounced in the patient with COVID-19 necrotizing leukoencephalopathy.

**ABBREVIATIONS:** COVID-19 = coronavirus disease 2019; DPL = delayed posthypoxic leukoencephalopathy; Lac = lactate; PEA = pulseless electrical activity; SAE = sepsis-associated encephalopathy; SARS-CoV-2 = Severe Acute Respiratory Syndrome coronavirus 2

Coronavirus disease 2019 (COVID-19), caused by Severe Acute Respiratory Syndrome coronavirus 2 (SARS-CoV-2), was declared a pandemic by the World Health Organization on March 11, 2020.<sup>1</sup> COVID-19 primarily affects the lower respiratory tract, but many organs can be involved, including the central nervous system.<sup>2,3</sup> Neurologic manifestations of SARS-CoV-2 infection are increasingly reported and include cerebrovascular complications, leukoencephalopathy, and other CNS disorders.<sup>4</sup> Although COVID-19-associated white matter abnormalities resemble other forms of diffuse white matter injury (such as posthypoxic leukoencephalopathy or sepsis-associated leukoencephalopathy), there are also notable differences, such as the neuroanatomic distribution of white matter lesions. The pathogenesis of COVID-19 white matter

abnormalities remains unknown, though “silent hypoxia” has been hypothesized to have a central role in their development.<sup>5,6</sup>

MR spectroscopy represents a noninvasive *in vivo* diagnostic tool for evaluating white matter injury and can provide valuable information regarding the underlying pathogenesis of white matter pathologies. In the setting of diffuse white matter injury, MR spectroscopy offers a complementary evaluation to structural MR brain imaging by providing a sensitive measurement of various *in vivo* metabolites. Most important, MR spectroscopy can identify neurochemical abnormalities even in the absence of corresponding findings on structural MR brain imaging.<sup>7,8</sup>

The metabolic profile of COVID-19-associated leukoencephalopathy using MRS has not been well established in the literature to date. We present examples of MR spectra in patients with COVID-19 and compare them with both other patients with leukoencephalopathy and a control.

Received June 14, 2020; accepted after revision August 13.

From the Departments of Radiology (O.R., A.W., K.E.-H., M.L.L., P.W.S., R.G.G., M.H.L., E.R.) and Neurology (B.L.E., D.F., S.S.M.), Massachusetts General Hospital and Harvard Medical School, Boston, Massachusetts; A.A. Martinos Center for Biomedical Imaging (A.W., A.T.-C., M.L.L., E.R.), Charlestown, Massachusetts; Ann & Robert H. Lurie Children’s Hospital of Chicago and Northwestern University Feinberg School of Medicine (S.J.M.) and Medical Image Analysis and Biometry Laboratory (A.T.-C.), Universidad Rey Juan Carlos, Madrid, Spain.

O. Rapalino and A. Weerasekera contributed equally to this article.

M.L. Loggia was funded by the National Institutes of Health grant 1R01NS095937-01A1.

Please address correspondence to Otto Rapalino, MD, Neuroradiology Division, Department of Radiology, Massachusetts General Hospital, 55 Fruit Street, GRB 273A Boston, MA 02114; e-mail: orapalino@mgh.harvard.edu

Indicates open access to non-subscribers at [www.ajnr.org](http://www.ajnr.org)

<http://dx.doi.org/10.3174/ajnr.A6877>

## Case Series

Six 3D multivoxel MRS datasets from 3 patients with COVID-19 (Fig 1 and Table 1), 2 control patients with leukoencephalopathy (posthypoxic and sepsis-related leukoencephalopathy), and 1 healthy age-matched control were acquired using 3T MR imaging scanners (Siemens, Erlangen, Germany). This 3D-MRS sequence was acquired using a Localization by Adiabatic Selective Refocusing (LASER) pulse sequence with a fast spiral *k*-space acquisition.<sup>9</sup> Acquisition parameters included the following: TE = 30 ms and 288 ms (except for the control and patient with delayed

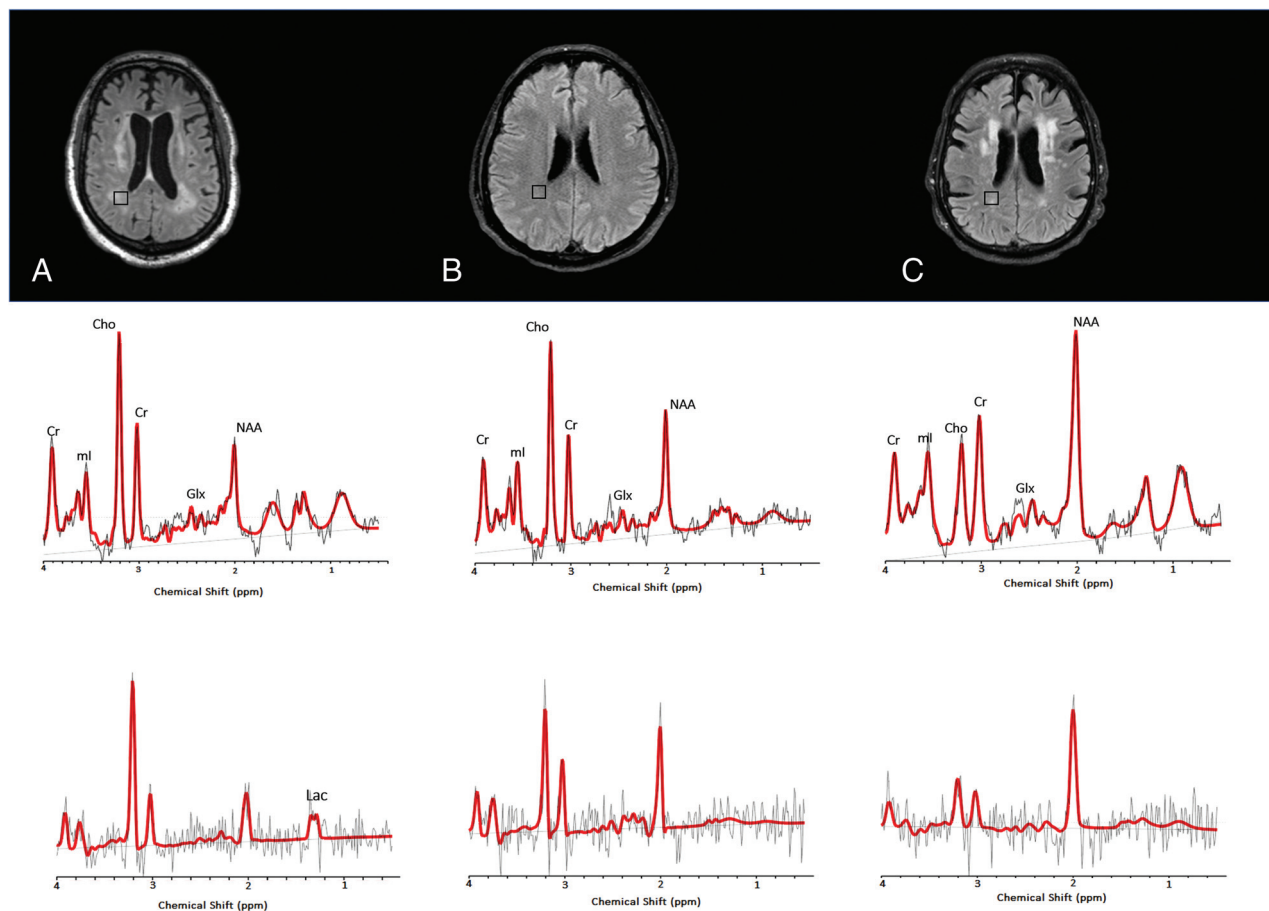


**FIG 1.**  $^1\text{H}$ -MR spectra of 3 consecutive patients with COVID-19. *Upper row:* Axial FLAIR images at the corona radiata level show representative MRS voxels (black squares) from sampled periventricular regions. *Lower row:* Corresponding spectrum (black) and LCMoel fit (red) from each patient acquired at TE = 30 ms (*upper row*) and TE = 288 ms (*lower row*). A, A patient with COVID-19-associated multifocal necrotizing leukoencephalopathy shows diffuse patchy WM lesions with markedly increased Cho and decreased NAA, as well as elevated Lac. B, A patient with COVID-19 after recent PEA cardiac arrest with subtle FLAIR hyperintense white matter changes also shows elevated Cho/Cr and decreased NAA/Cr ratios. However, these derangements are less severe than in the patient in A. There is no clear elevation of Lac. C, A patient with COVID-19 without encephalopathy or recent severe hypoxia has normal Cho/Cr, with mildly decreased NAA/Cr and no lactate elevation. Cho, Choline; NAA, N-Acetyl-Aspartate; ml, Myo-Inositol; Lac, Lactate; Glx, Glutamate + Glutamine.

**Table 1: Demographics and clinical information**

| Subject | Diagnosis   | Status  | Age (yr) | Sex |
|---------|---|---|----------|-----|
| COVID-A | COVID-19-related multifocal necrotizing leukoencephalopathy                   | ICU and intubated                               | 63       | M   |
| COVID-B | COVID-19-related recent PEA cardiac arrest, without clear leukoencephalopathy | ICU and intubated                               | 53       | M   |
| COVID-C | COVID-19 without clear leukoencephalopathy or recent severe hypoxia           | Neurology ward and not intubated                | 72       | M   |
| DPL     | Non-COVID-19 delayed posthypoxic/toxic leukoencephalopathy                    | Neurology ward and not intubated                | 44       | F   |
| SAE     | Non-COVID-19 presumed sepsis-associated encephalopathy                        | ICU and mechanical ventilation via tracheostomy | 55       | F   |
| Control | Healthy volunteer   |   | 65       | M   |

**Note:**—ICU indicates intensive care unit.

posthypoxic leukoencephalopathy [DPL]), TR = 1500 ms, Number of Acquisitions = 5, isotropic resolution 1 cc. Excitation VOIs were placed using FLAIR or T2-weighted images to include the white matter abnormalities.

Raw data files were processed using the LCMoel software package, Version 6.3 (<http://www.lcmoel.com/>) with the appropriate

basis set.<sup>10</sup> For the data analysis, 6–8 white matter MR spectroscopy voxels of the section with the most prominent white matter abnormalities were chosen, and their metabolite ratios were averaged.

Of the patients with COVID-19, 1 patient had MR imaging findings compatible with a necrotizing leukoencephalopathy with abnormal reduced diffusivity and cavitation within the white matter

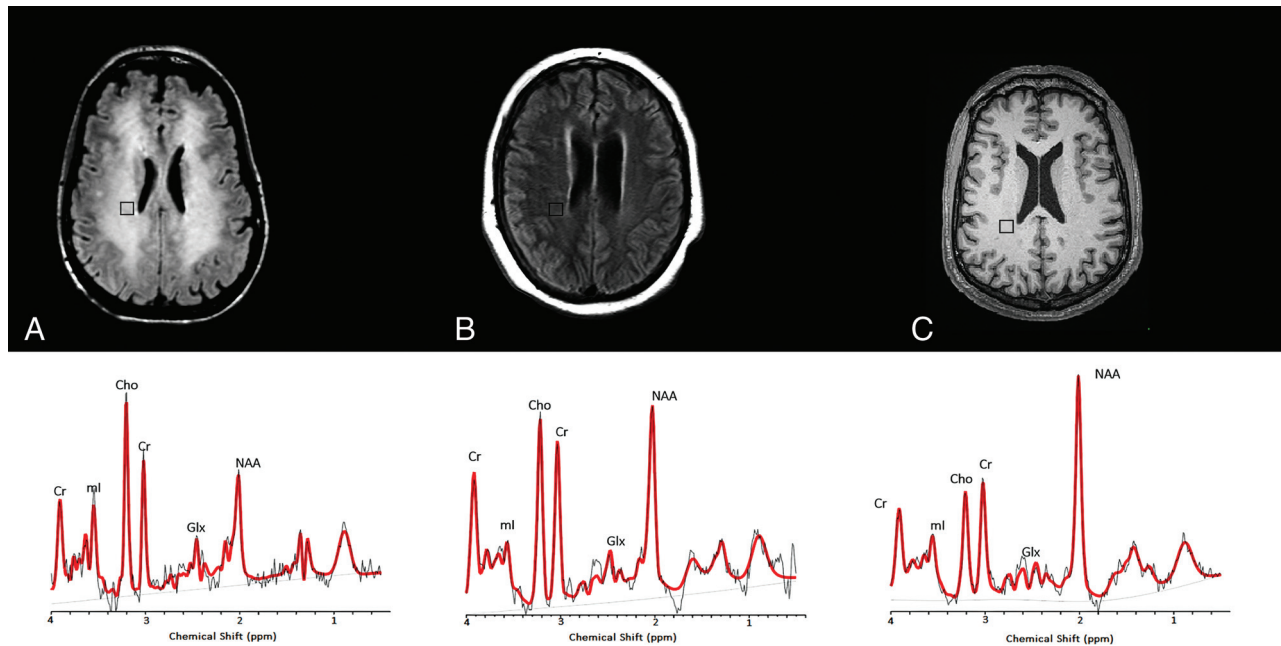


**FIG 2.** <sup>1</sup>H-MR spectra from 2 non-COVID leukoencephalopathy patients, compared with a spectrum from a healthy control patient. *Upper row:* Axial noncontrast FLAIR (A and B) and T1-weighted (C) images at the level of the corona radiata show representative MRS voxels (black squares) from sampled periventricular regions. *Lower row:* Corresponding spectrum (black) and LCMoel fit (red) from each patient acquired at TE = 30 ms. A, A patient with delayed posthypoxic/toxic leukoencephalopathy shows an increase of Cho/Cr and decreased NAA/Cr ratios. B, A patient with sepsis-associated encephalopathy shows milder degrees of Cho/Cr elevation and NAA/Cr reduction. C, A healthy control subject with a normal MR spectrum. Cho, Choline; NAA, N-Acetyl-Aspartate; ml, Myo-Inositol; Lac, Lactate; Glx, Glutamate + Glutamine.

**Table 2: Mean, SD, and percentage difference relative to controls of brain MRS metabolite ratios in 3 patients with and 3 patients without COVID-19<sup>a</sup>**

| Subject | No. Voxels | NAA/Cr <sup>b</sup>             | Cho/Cr <sup>b</sup>             | ml/Cr <sup>b</sup>              | Glx/Cr <sup>b</sup>             | Lac/Cr <sup>c</sup> |
|---------|------------|---------------------------------|---------------------------------|---------------------------------|---------------------------------|---------------------|
| COVID-A | 7          | 0.61 ± 0.13 (−85%) <sup>d</sup> | 0.65 ± 0.05 (+80%) <sup>d</sup> | 1.17 ± 0.07 (+39%) <sup>d</sup> | 1.46 ± 0.20 (+51%) <sup>d</sup> | 0.76 ± 0.1          |
| COVID-B | 8          | 1.10 ± 0.15 (−33%) <sup>d</sup> | 0.54 ± 0.04 (+63%) <sup>d</sup> | 1.16 ± 0.09 (+38%) <sup>d</sup> | 1.40 ± 0.13 (+47%) <sup>d</sup> | 0                   |
| COVID-C | 6          | 1.47 ± 0.08 (−5%)               | 0.27 ± 0.03 (−4%)               | 1.23 ± 0.10 (+44%) <sup>d</sup> | 1.04 ± 0.22 (+18%)              | 0                   |
| DPL     | 8          | 0.81 ± 0.11 (−62%) <sup>d</sup> | 0.48 ± 0.02 (+53%) <sup>d</sup> | 1.09 ± 0.05 (+32%) <sup>d</sup> | 1.82 ± 0.14 (+71%) <sup>d</sup> |                     |
| SAE     | 7          | 0.95 ± 0.16 (−47%) <sup>d</sup> | 0.32 ± 0.04 (+13%)              | 0.61 ± 0.06 (−26%)              | 1.10 ± 0.12 (+23%)              | 0                   |
| Control | 6          | 1.54 ± 0.17                     | 0.28 ± 0.04                     | 0.79 ± 0.04                     | 0.87 ± 0.07                     |                     |

<sup>a</sup> Positive and negative percentages between parentheses indicate percentage difference compared to the control subject.

<sup>b</sup> Data measured on short-TE (TE = 30 ms) spectra.

<sup>c</sup> Data measured on long-TE (TE = 288 ms) spectra. No long-TE spectra were available for the DPL and control cases.

<sup>d</sup> Percentage differences of >30% in magnitude. The distribution of these metabolite ratio derangements in patients with COVID-A (leukoencephalopathy) and COVID-B (post-cardiac arrest) is similar to that of the patient with DPL.

lesions (COVID-A) (Fig 1A). The second patient had pulseless electrical activity (PEA) arrest while in the intensive care unit and subsequently developed altered mental status. His MR imaging showed cerebellar cortical and hippocampal signal abnormalities suggestive of prior hypoxic-ischemic injury and subtle bilateral cerebellar and supratentorial white matter T2/FLAIR hyperintensities (COVID-B) (Fig 1B). The third patient with COVID-19 without an encephalopathic syndrome had a history of parkinsonism and developed catatonia of unclear etiology (COVID-C) (Fig 1C). This patient's MR imaging showed mild nonspecific periventricular and deep white matter changes suggestive of small-vessel disease (considering their neuroanatomic distribution). None of these patients were found to have other neurologic comorbidities (eg, other metabolic encephalopathies, hydrocephalus, and so forth).

Data from these 3 patients were contrasted to multivoxel MRS data obtained before the COVID-19 pandemic from 2 patients with

other leukoencephalopathies. One patient had DPL and developed severe encephalopathy, rigidity, and mutism, likely related to a prior toxic exposure (opiates) or a hypoxic episode (Fig 2A). The other patient without COVID-19 had sepsis-associated encephalopathy (SAE), with mild diffuse white matter abnormalities on brain MR imaging studies (Fig 2B).

Last, data of all 5 patients with leukoencephalopathy were compared with a dataset acquired using the same protocol from a healthy control subject, a 65-year-old man who volunteered for a research study (Fig 2C).

MRS datasets with short TEs (TE = 30 ms) were analyzed to quantify ratios of NAA, Cho, ml, and Glx relative to Cr. Lactate (Lac)/Cr levels were quantified using MRS datasets with long TEs (TE = 288 ms). Table 2 summarizes the means, SDs, and percentage differences of metabolite levels compared with the control.

Comparative analysis showed decreased NAA/Cr levels within the white matter in 2 of the patients positive for COVID-19 compared with the control. The patient with necrotizing leukoencephalopathy (COVID-A) had the most diminished NAA levels, which were completely absent in several MR spectroscopy voxels, followed by the patient with recent cardiac arrest and mild diffuse white matter changes without necrosis (COVID-B). The patient with COVID-C without recent cardiac arrest or overt leukoencephalopathy (Fig 1) had slightly decreased NAA/Cr levels compared with the age-matched control. The metabolic profiles of the 3 patients with COVID-19 were contrasted to those of 2 patients with other leukoencephalopathies without COVID-19 (described above) (Fig 2). The NAA/Cr levels of these patients without COVID leukoencephalopathy were also decreased but still higher than those in the patient with COVID-A (Table 2).

Compared with the control, 2 of the 3 patients with COVID-19 had elevated Cho/Cr levels (Table 2). The third patient with COVID-19 without leukoencephalopathy (COVID-C) showed Cho/Cr levels indistinguishable from those of the control. The patient without COVID-19 with DPL and extensive white matter abnormalities showed increased Cho/Cr ratios, while the patient with SAE had a relatively normal range of Cho/Cr ratios.

All 3 patients with COVID-19 and the patient without COVID-19 with DPL showed elevated mI/Cr levels (Table 2). Most interesting, our patient with sepsis-associated encephalopathy had decreased mI/Cr ratios. Glx/Cr was markedly increased in the 2 patients with COVID-19 with necrotizing leukoencephalopathy and after cardiac arrest as well as in the patient without COVID-19 with DPL. Lac/Cr ratios were increased in the patient with COVID-19 with necrotizing leukoencephalopathy on long-TE spectra. No elevation of Lac/Cr ratios was seen in the patient with SAE. The patient with DPL and control did not have long-TE spectra. Therefore, we cannot confirm or exclude the presence of lactate in these subjects (Fig 2A).

## DISCUSSION

Multiple recent reports in the medical literature have confirmed the development of leukoencephalopathy as a potential CNS complication in SARS-CoV-2 infection,<sup>11,12</sup> though no study has reported the MR spectroscopic findings in these patients. We evaluated the metabolic differences among 3 patients with COVID-19 (1 with necrotizing leukoencephalopathy, another after cardiac arrest, and the third with mild nonspecific white matter changes without clinical encephalopathy) and other control groups with multivoxel MR spectroscopy to better understand the underlying pathophysiology of this disease. Markedly increased Cho/Cr, decreased NAA/Cr, and increased Lac/Cr ratios were observed in the patient with COVID-19 with multifocal necrotizing leukoencephalopathy. Less pronounced changes in Cho/Cr and NAA/Cr ratios were noted in the patient with COVID-19 with prior PEA arrest and subtle nonspecific white matter signal abnormalities. Notably, the magnitude of the Cho and NAA abnormalities in the patient with COVID-19 associated necrotizing leukoencephalopathy was more pronounced compared with the patients with delayed post-hypoxic leukoencephalopathy and SAE.

In our series, similar patterns of metabolic changes were observed in the setting of COVID-19-associated

leukoencephalopathy and DPL, namely elevated Cho, elevated Lac, decreased NAA, increased mI, and increased Glx ratios in relation to Cr. This spectral pattern has been previously reported in the setting of DPL following carbon monoxide poisoning or medication overdose.<sup>13-15</sup> Prolonged impaired oxygenation to the subcortical white matter is thought to promote anaerobic metabolism and leads to elevated tissue Lactate.<sup>14,15</sup>

The observed increase of Cho/Cr ratios in the patients with leukoencephalopathy, particularly in the case of COVID-associated necrotizing leukoencephalopathy, likely reflects demyelination within these white matter lesions as recently described in an initial neuropathologic study of a patient with COVID-19.<sup>16</sup> Cho elevation could also be related to cell death and/or immune cellular infiltration within areas of demyelination.<sup>17</sup> Axonal damage was also reported on pathology<sup>16</sup> and likely contributes to the decreased NAA/Cr ratios we observed.

Increased levels of Myo-Inositol (mI) may reflect neuroinflammation, which when coupled with choline elevations in demyelinating pathologies may reflect glial proliferation.<sup>18</sup> The presence of elevated Glx levels has been reported in cases of acute excitotoxic leukoencephalopathy<sup>19</sup> and viral-associated acute leukoencephalopathy with restricted diffusion.<sup>20</sup> Both conditions are thought to be mediated by excitotoxic injury to the cerebral white matter and exhibit prominent reduced diffusivity within white matter lesions.

Notably, the metabolic derangements seen in the setting of COVID-19-associated multifocal necrotizing leukoencephalopathy are similar to those observed with DPL. However, more evidence is required to validate this conclusion. Some of the previously published MR spectroscopy studies of necrotizing encephalopathies from other etiologies<sup>21</sup> also showed increased Lac along with decreased NAA and increased Cho,<sup>22</sup> while others showed Glx and lipid elevations predominantly.<sup>23</sup> Certainly, additional research is warranted in this new field of COVID-19-related metabolic derangement.

The small patient cohort of our study limits our ability to generalize our observations. MRS was only performed in patients with SARS-CoV-2 infection when requested by referring providers for specific clinical indications. Furthermore, the controls without COVID-19 are slightly younger, especially the patient with DPL. Another limitation of our study is that only a single time point was assessed; thus, we cannot exclude other baseline conditions before the SARS-CoV-2 infection, such as chronic small-vessel disease, that may affect our results. Finally, some of these subjects (the patient with DPL and the healthy control) did not have a long-TE MRS acquisition, limiting our ability to unequivocally determine the presence or absence of Lac.

In conclusion, the reported spectroscopic abnormalities within the white matter lesions of COVID-19-associated leukoencephalopathy may reflect several pathophysiologic processes, including but not limited to the following: 1) an anaerobic metabolic environment produced by the well-described “silent hypoxia” seen in these patients, resulting in elevation of Lac levels; 2) neuronal dysfunction and axonal injury with decreased NAA/Cr ratios; and 3) increased membrane destruction or turnover with elevated Cho/Cr ratios. Continued data collection in a larger cohort is required to



validate these observations and better elucidate their significance in the pathophysiology of SARS-CoV-2 infection.

Disclosures: Otto Rapalino—UNRELATED: Travel and hotel expenses as a lecturer at an event were sponsored by GE Healthcare in August 2019. This lecture did not have any commercial content and did not have any relationship to the current work. Brian L. Edlow—RELATED: Grant: James S. McDonnell Foundation, Comments: McDonnell Foundation COVID-19 Recovery of Consciousness Consortium.\* David Fischer—RELATED: Grant: R25NS06574309. Shibani Mukerji—UNRELATED: Grants/Grants Pending: National Institute of Mental Health, Comments: K23MH115812.\* Michael H. Lev—UNRELATED: Consultancy: Takeda Pharmaceutical Company, GE Healthcare, Comments: Consultant; Grants/Grants Pending: National Institutes of Health, Comments: Coinvestigator on 2 technical development grants; Patents (Planned, Pending or Issued): Electrical Impedance Spectroscopy, Artificial Intelligence-related. Eva-Maria Ratai—UNRELATED: Employment: Massachusetts General Hospital; Grants/Grants Pending: National Institutes of Health, National Science Foundation, Comments: R01NS080816, R01HD065762, R01HD085813, U01NS104326, R01DA047088, P01-AT009965, R01CA190901, R01NS112694.\* Marco L. Loggia—RELATED: Grant: National Institute of Neurological Disorders and Stroke, Comments: 1R01NS095937-01A1\*; UNRELATED: Grants/Grants Pending: National Institutes of Health. Angel Torrado-Carvajal—UNRELATED: Employment: Universidad Rey Juan Carlos, Assistant Professor (September 2019 until now); Massachusetts General Hospital, Research Fellow (August 2017 to August 2019); Grants/Grants Pending: Comunidad de Madrid, MIMC3 PET/MR Project.\* \*Money paid to the institution.

## REFERENCES

1. Cucinotta D, Vanelli M. **WHO declares COVID-19 a pandemic.** *Acta Biomed* 2020;91:157–60 [CrossRef Medline](#)
2. Berlin DA, Gulick RM, Martinez FJ. **Severe Covid-19.** *N Engl J Med* 2020 May 15. [Epub ahead of print] [CrossRef Medline](#)
3. Romero-Sanchez CM, Diaz-Maroto I, Fernandez-Diaz E, et al. **Neurologic manifestations in hospitalized patients with COVID-19: the ALBA COVID registry.** *Neurology* 2020;95:e1060–70 [CrossRef Medline](#)
4. Helms J, Kremer S, Merdji H, et al. **Neurologic features in severe SARS-CoV-2 infection.** *N Engl J Med* 2020;382:2268–70 [CrossRef Medline](#)
5. Couzin-Frankel J. **The mystery of the pandemic's 'happy hypoxia.'** *Science* 2020;368:455–56 [CrossRef Medline](#)
6. Solomon IH, Normandin E, Bhattacharyya S, et al. **Neuropathological features of Covid-19.** *N Engl J Med* 2020;383:989–92 [CrossRef Medline](#)
7. Sun J, Song H, Yang Y, et al. **Metabolic changes in normal appearing white matter in multiple sclerosis patients using multivoxel magnetic resonance spectroscopy imaging.** *Medicine (Baltimore)* 2017;96:e6534 [CrossRef Medline](#)
8. Bizzi A, Castelli G, Bugiani M, et al. **Classification of childhood white matter disorders using proton MR spectroscopic imaging.** *AJNR Am J Neuroradiol* 2008;29:1270–75 [CrossRef Medline](#)
9. Andronesi OC, Gagoski BA, Sorensen AG. **Neurologic 3D MR spectroscopic imaging with low-power adiabatic pulses and fast spiral acquisition.** *Radiology* 2012;262:647–61 [CrossRef Medline](#)
10. Provencher SW. **Automatic quantitation of localized in vivo 1H spectra with LCModel.** *NMR Biomed* 2001;14:260–64 [CrossRef Medline](#)
11. Radmanesh A, Derman A, Lui YW, et al. **COVID-19-associated diffuse leukoencephalopathy and microhemorrhages.** *Radiology* 2020 May 21. [Epub ahead of print] [CrossRef Medline](#)
12. Sachs JR, Gibbs KW, Swor DE, et al. **COVID-19-associated leukoencephalopathy.** *Radiology* 2020;296:E184–85 [CrossRef Medline](#)
13. Beeskov AB, Oberstadt M, Saur D, et al. **Delayed post-hypoxic leukoencephalopathy (DPHL): an uncommon variant of hypoxic brain damage in adults.** *Front Neurol* 2018;9:708 [CrossRef Medline](#)
14. Shprecher DR, Flanigan KM, Smith AG, et al. **Clinical and diagnostic features of delayed hypoxic leukoencephalopathy.** *J Neuropsychiatry Clin Neurosci* 2008;20:473–77 [CrossRef Medline](#)
15. Terajima K, Igarashi H, Hirose M, et al. **Serial assessments of delayed encephalopathy after carbon monoxide poisoning using magnetic resonance spectroscopy and diffusion tensor imaging on 3.0T system.** *Eur Neurol* 2008;59:55–61 [CrossRef Medline](#)
16. Reichard RR, Kashani KB, Boire NA, et al. **Neuropathology of COVID-19: a spectrum of vascular and acute disseminated encephalomyelitis (ADEM)-like pathology.** *Acta Neuropathol* 2020;140:1–6 [CrossRef Medline](#)
17. Brenner RE, Munro PM, Williams SC, et al. **The proton NMR spectrum in acute EAE: the significance of the change in the Cho:Cr ratio.** *Magn Reson Med* 1993;29:737–45 [CrossRef Medline](#)
18. Bitsch A, Bruhn H, Vougioukas V, et al. **Inflammatory CNS demyelination: histopathologic correlation with in vivo quantitative proton MR spectroscopy.** *AJNR Am J Neuroradiol* 1999;20:1619–27 [Medline](#)
19. Takanashi JI, Murofushi Y, Hirai N, et al. **Prognostic value of MR spectroscopy in patients with acute excitotoxic encephalopathy.** *J Neurol Sci* 2020;408:116636 [CrossRef Medline](#)
20. Kamate M. **Acute leukoencephalopathy with restricted diffusion.** *Indian J Crit Care Med* 2018;22:519–23 [CrossRef Medline](#)
21. Premji S, Kang L, Rojiani MV, et al. **Multifocal necrotizing leukoencephalopathy: expanding the clinicopathologic spectrum.** *J Neuropathol Exp Neurol* 2019;78:340–47 [CrossRef Medline](#)
22. Raghavendra S, Nair MD, Chemmanam T, et al. **Disseminated necrotizing leukoencephalopathy following low-dose oral methotrexate.** *Eur J Neurol* 2007;14:309–14 [CrossRef Medline](#)
23. Aydin H, Ozgul E, Agildere AM. **Acute necrotizing encephalopathy secondary to diphtheria, tetanus toxoid and whole-cell pertussis vaccination: diffusion-weighted imaging and proton MR spectroscopy findings.** *Pediatr Radiol* 2010;40:1281–84 [CrossRef Medline](#)